Electrochimica Acta 331 (2020) 135428

Contents lists available at ScienceDirect

Electrochimica Acta

journal homepage: www.elsevier.com/locate/electacta

Stainless steel in simulated milk and whey protein solutions – Influence of grade on corrosion and metal release

Masoud Atapour [a, b, *], Inger Odnevall Wallinder [a], Yolanda Hedberg [a, **]

[a] KTH Royal Institute of Technology, School of Engineering Sciences in Chemistry, Biotechnology and Health, Dept. Chemistry, Div. Surface and Corrosion Science, SE-10044, Stockholm, Sweden
[b] Department of Materials Engineering, Isfahan University of Technology, Isfahan, 84156-83111, Iran

ARTICLE INFO

Article history:
Received 9 October 2019
Received in revised form
26 November 2019
Accepted 30 November 2019
Available online 3 December 2019

Keywords:
Surface oxide
Complexation
Pitting corrosion
Food safety
Biocorrosion

ABSTRACT

Reactions at the biointerfaces between stainless steel and protein-rich dairy products, which contain whey proteins, are important to consider in terms of food safety and material grade selection. Changes in corrosion behavior, metal release, and surface composition of austenitic (AISI 316 L), ferritic (AISI 430), and lean duplex (LDX 2101) stainless steels in simulated milk (SMS) and whey protein solution were investigated. The amount of released metals and the corrosion susceptibility increased according to 2101 < 316 L < 430. All grades revealed low corrosion rates in the whey protein solution without any sign of active/metastable corrosion. Pitting corrosion was evident for 430 in SMS. The total amount of released metals (iron, chromium, and nickel) was significantly higher in whey protein solution compared with SMS. This suggests the metal release process to be mainly governed by complexation reactions. Nickel was preferentially released compared to its bulk composition fraction for both 316 L and 2101 in the highly complexing SMS. Reduced metal release rates with time correlated with the enrichment of chromium in the surface oxide. The extent of metal release was for all metals substantially lower than release limits of metals stipulated in health regulations related to the use of alloys and metals in food-related environments.

1. Introduction

Stainless steel alloys (SS) are increasingly used in food contact applications due to their superior mechanical properties combined with low corrosion rates [1]. Data on metal release (migration) from stainless steel used in transportation or processing containers is nonetheless relatively scarce, in particular for protein-containing solutions of relevance for food and beverages [2]. The global demand for protein-based products has increased due to increasing population and improved average living standards [3]. Bovine milk is a common protein source for humans, with an increased annual consumption of 3.3% in the developing countries from the early 1990s until today [4]. Dairy products are considered important protein-containing food sources due to their functional and nutritive characteristics. The main proteins of milk are casein and whey proteins present in a ratio of 5:1 [5]. Whey proteins are also ingredients of different protein products, e.g. protein drinks, which are increasingly used in connection to sport activities and fitness lifestyles [6]. There is hence an increasing demand on food safety related to the use and performance of materials used for storage, transport and processing [7].

Stainless steels are established main structural materials in the food and dairy industry [8]. It has been reported that stainless steels may suffer from pitting corrosion in milk processing plants and related equipment [9]. Among the austenitic stainless steel grades used in food processing, AISI 304 and AISI 316 are most common [10]. Although grade 316 is the more corrosion resistant grade, severe corrosion cases have been reported for this grade when used in inappropriate environments [10]. The authors have recently performed metal release studies for austenitic stainless steel (grade AISI 316 L) in simulated milk solutions and whey protein solution under static and stirring conditions [11]. The study concluded that the presence of whey proteins and friction in a synergistic way increased the amount of released metals. Active corrosion of stainless steels in food contact is very rare, and when reported,

* Corresponding author. KTH Royal Institute of Technology, School of Engineering Sciences in Chemistry, Biotechnology and Health, Dept. Chemistry, Div. Surface and Corrosion Science, SE-10044, Stockholm, Sweden.
** Corresponding author.
E-mail addresses: m.atapour@cc.iut.ac.ir (M. Atapour), yolanda@kth.se (Y. Hedberg).

https://doi.org/10.1016/j.electacta.2019.135428

found to be mostly related to inappropriate grade selection for the given environment, faulty fabrication or design, and/or incorrect cleaning procedures [10]. Such conditions may also negatively affect the organoleptic aspects of the food and food safety [12]. Duplex stainless steels have been considered as more corrosion-resistant within the food industry and therefore in some cases been implemented as alternatives [10]. Ferritic stainless steels, such as AISI 430, are used in some food equipment, such as kitchen utensils [13], and have been suggested as nickel-free alternatives, however, their corrosion rates are higher as compared to the other grades mentioned [10].

The extent of metal release (migration) from stainless steel in food environments is governed by different mechanisms and processes including corrosion (metal oxidation), pitting corrosion, and complexation-induced metal release [14–23]. It has been hypothesized that *i*) metal release is preceded and triggered by the adsorption of proteins [24], *ii*) protein exchange might increase (and in some cases reduce) the extent of corrosion [20,25], *iii*) adsorbed proteins can act as beneficial lubricants in the case of wear processes [26], and *iv*) that the adsorption of proteins can contribute to the mechanisms of tribocorrosion via complexation with metals within the surface oxide [11].

To the best of our knowledge, there is no study that addresses both metal release and corrosion of different stainless steel grades in simulated milk compared with whey protein solutions. Such an investigation is relevant to ensure correct grade selection and have control of potential interactions between the container material and its environment. The aim of this study was therefore to elucidate the interactions between a whey protein solution and stainless steel surfaces of different grade and microstructure compared with their behavior in a non-protein containing simulated milk solution. This was performed by using electrochemical-, spectroscopic- and microscopic techniques to study changes in the corrosion performance, extent of metal release, and surface composition for austenitic (AISI 316 L), ferritic (AISI 430), and lean duplex (LDX 2101) stainless steels.

2. Materials and methods

2.1. Materials and microstructure

Austenitic AISI 316 L (denoted 316 L), ferritic AISI 430 (430) and duplex EN 1.4162 (2101) stainless steel sheets (2 mm thick) were provided by the International Stainless Steel Forum, Belgium. Their nominal bulk composition is given in Table 1 (detailed data for 316 L is given in Ref. [11]). The microstructure of the grades was highlighted by means of light optical microscopy (LOM), using a Leica DM2700 M instrument. Coupons were polished in steps down to 0.25 μm (diamond paste) followed by chemical etching at room temperature at different conditions to visualize the microstructure; 316 L (20 s in 10 mL nitric acid, 15 mL hydrochloric acid, 10 mL acetic acid and two drops of glycerin), 430 (20 s in 50 mL hydrochloric acid, 100 mL water and 8.33 g $FeCl_3 \cdot 6H_2O$) and 2101 (30 s in 30 mL hydrochloric acid, 70 mL water, and 1 g $K_2S_2O_5$). The etched coupons were cleaned using ultrapure water (18.2 MΩ cm, Millipore, Solna, Sweden), and dried with nitrogen gas at room temperature prior to the microscopic examination. Phase fractions of the 2101 grade were determined using the Clemex image tool.

2.2. Experimental conditions

Coupons of all grades, sized 15 mm × 15 mm, were prepared as described earlier [11]. In short, the coupons were abraded (both sides and all edges) using 1200 SiC grit paper (with water), ultrasonically cleaned by acetone and ethanol for 5 min, dried with nitrogen gas at room temperature, and aged (stored) for 24 ± 1 h in a desiccator at room temperature (25 ± 2 °C). This procedure enables reproducibility due to a constant surface history, as the time between grinding/polishing and experiments largely influences the metal release and corrosion results [27].

Whey protein isolate (Lacprodan DI-9224) with a total protein content of at least 92% was obtained from Arla Food Ingredients, Denmark.

The test solutions were prepared as described in Ref. [11]. In short, one day prior to each exposure, 80 g/L whey protein (typical for whey protein drinks) was freshly dispersed in ultrapure water and stored for 24 ± 1 h in a refrigerator (4 °C). Simulated milk solution (SMS) was prepared from ultrapure water and analytical grade reagents (1.57 g/L KH_2PO_4, 1 g/L $K_3C_6H_5O_7 \cdot H_2O$, 1.42 g/L $Na_3C_6H_5O_7 \cdot 2H_2O$, 0.18 g/L K_2SO_4, 0.3 g/L K_2CO_3, 0.6 g/L KCl, 1.32 $CaCl_2 \cdot 2H_2O$ and 0.65 g/L $MgCl_2 \cdot 6H_2O$). The pH of the SMS and the whey protein solution was 6.8. Triplicate coupons and one blank sample (test solution only) were exposed in parallel for each grade and test condition at room temperature for 0.5, 4, 24, and 48 h, respectively. All vessels and tools were acid-cleaned in 10 vol-% HNO_3 for at least 24 h, rinsed four times in ultrapure water and dried in ambient laboratory air. The pH of all test solutions was measured prior to and after exposure. After immersion, the coupons were rinsed with 1 mL ultrapure water, dried with nitrogen gas at room temperature, and placed in a desiccator before post-evaluations using X-ray photoelectron spectroscopy (XPS), LOM, and scanning electron microscopy (SEM).

The whey solution samples were frozen and the SMS solution samples were acidified with ultrapure 65 vol-% nitric acid (pH < 2) and stored at room temperature (at most one month) before solution analysis. The whey solutions were digested prior to the atomic absorption spectroscopy (AAS) measurements as described in Ref. [11].

2.3. Atomic absorption spectroscopy (AAS) analysis and presentation of data

Total amounts of released Fe, Cr and Ni were determined in the acidified SMS and the digested whey protein solutions by means of graphite furnace AAS (PerkinElmer AA800), details given in Ref. [11]. The limits of detection, LODs, determined from three times the average standard deviation of all blank solutions were 8.6 μg Fe/L, 0.48 μg Cr/L and 2.0 μg Ni/L for the whey protein solution, and 2.3 μg Fe/L, 0.77 μg Cr/L and 1.5 μg Ni/L for SMS. Background metal concentrations were determined to <25 μg Fe/L and

Table 1
Microstructure and nominal bulk alloy composition of stainless steel grades 316 L, 430 and 2101 based on supplier information (wt.%).

Grade	UNS	EN	Microstructure	Fe	Cr	Mn	Ni	Cu	Mo	N	C	S
AISI 316 L	S31603	1.4404	Austenitic	Bal.	16.9	1.3	10.1	0.5	2.0	0.05	0.02	0.0006
AISI 430	S43000	1.4016	Ferritic	Bal.	16.0	0.3	0.1	0.04	0.02	0.03	0.03	0.0016
EN 1.4162	S32101	1.4162	Duplex	Bal.	21.4	4.8	1.6	0.3	0.28	0.22	0.02	0.0010

<LOD (Cr and Ni) for the whey solution, and <LOD (Cr and Fe) and <4.7 μg Ni/L for the SMS solution. Traces of Fe in the whey protein are expected and known from previous studies [11]. The corresponding blank concentrations were subtracted from the sample concentrations. These corrected concentrations were multiplied by the exposure volume and any dilution factor (for digested samples only), divided by the exposed coupon area as described in Ref. [11], and reported as the released amount of metals in μg cm^{-2}. Mean values are reported with standard deviations of independent triplicate samples.

2.4. Electrochemical measurements

Electrochemical measurements were carried out in a conventional three-electrode flat cell with the stainless steel coupons (exposed area 1 cm^2) as working electrodes, a platinum mesh as counter electrode and an Ag/AgCl saturated KCl electrode as reference electrode. Solution- and coupon preparation were as described above. All electrochemical measurements were conducted at aerated conditions and room temperature using a Princeton Applied Research potentiostat equipped with several PMC-1000 channels, allowing parallel independent measurements. Open circuit potential (OCP), potentiodynamic polarization and electrochemical impedance spectroscopy (EIS) measurements were carried out in both the whey protein solution and in SMS. OCP measurements were performed for 4 h before all other electrochemical measurements were conducted. Potentiodynamic polarization measurements were performed from −0.25 V vs. OCP to 1.6 V vs. Ag/AgCl sat. KCl with a scan rate of 1 mV s^{-1}. EIS was performed at OCP with an amplitude of 10 mV_{rms} sweeping frequencies from 10,000 Hz−0.01 Hz.

The Randles electrical-equivalent circuit (EEC) (R_S ($R_{p\text{-}EIS}Q$)) was used to fit the EIS data. R_s is the resistance of the electrolyte between the working and the reference electrode. R_p and the constant phase element (CPE) represent the resistance and capacitance of the barrier (passive) layer, respectively. Due to the presence of surface roughness and non-homogeneities of the coupon surfaces, CPE was used instead of a pure capacitor [28]. CPE is defined as:

$$Z_{CPE} = 1 \Big/ (jw)^0 Y_0 \quad (1)$$

where $j = \sqrt{-1}$, n is the CPE exponent that represents the deviation from a pure capacitance, Y_0 is designated as the general admittance function and ω is the angular frequency with $\omega = 2\pi f$. CPE can describe several elements: $n = 1$ represents a perfect capacitance, $n = 0.5$ shows a Warburg impedance and $n = 0$ corresponds to a resistance.

2.5. XPS characterization

Surface compositional analysis of the outermost surface (approx. 5−10 nm) was performed on duplicate locations of both unexposed and selected exposed coupons using X-ray photoelectron spectroscopy (XPS, UltraDLD spectrometer, Kratos Analytical, monochromatic 150 W, Al X-ray source on areas sized 700 × 300 μm^2). Wide and high-resolution spectra (pass energy 20 eV) for Fe 2p, Cr 2p, Ni 2p, P 2p, Cl 2p, N 1s, O 1s, and C 1s were collected. All binding energies were corrected to the C 1s peak at 285.0 eV. The $2p_{3/2}$ peaks of Fe and Cr were separated into their metallic (Fe: 707.3 ± 0.2 eV; Cr: 574.4 ± 0.3 eV) and oxidic (Fe: 711.3 ± 0.4 eV; Cr: 577.0 ± 0.3 eV) fractions to quantify their relative amounts. Ni (2p) was only observed in its metallic state (853.1 ± 0.1 eV).

3. Results and discussion

3.1. Metallographic investigation

Differences in microstructure of the austenitic 316 L, ferritic 430 and duplex 2101 stainless steels are visualized in Fig. 1 using LOM images. 316 L showed the presence of fine equiaxed grains (average grain size of 8 μm) of austenite with some annealing twins, Fig. 1a. As expected, no chromium carbides were observed in the grain boundaries. The microstructure of grade 430 revealed coarse grains of ferrite sized 15 ± 4 μm and the presence of non-uniformly distributed carbides (Fig. 1b). As shown in Fig. 1c, the microstructure of grade 2101 showed elongated austenitic (γ) areas (bright) in a matrix (dark) of ferrite (α). Quantitative metallography revealed approximately similar volume fractions of the γ- (51 ± 2) and the α- (49 ± 2) phase.

3.2. OCP measurements

Changes in OCP with time up to 4 h in SMS are presented in Fig. 2 (top) for two independent replicate coupons of 316 L, 430 and 2101. The OCP was slightly reduced with time for all grades with a large drop only observed for grade 430 after approximately 2−2.5 h in SMS. This drop in potential was most probably related to a (metastable) pitting corrosion event, see next section. In whey protein solution, Fig. 2 (bottom), relatively constant and

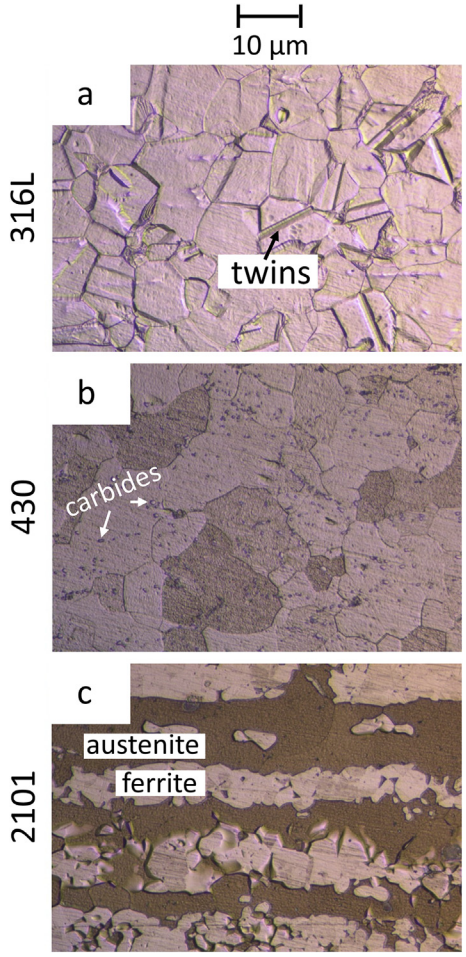

Fig. 1. LOM images of etched stainless steels grades at different magnification: (a) 316 L; (b) 430; (c) 2101.

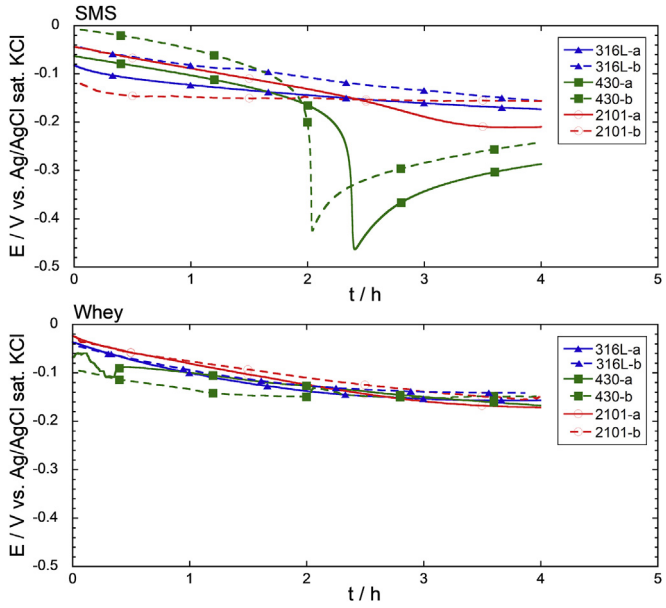

Fig. 2. Open-circuit potential for duplicate coupons of 316 L, 430 and 2101 immersed for 4 h in in SMS (top) and whey protein solution (bottom).

comparable potential levels were determined for the different grades after 4 h of immersion.

3.3. Potentiodynamic polarization measurements

Representative potentiodynamic polarization curves are presented in Fig. 3 for the stainless steel grades after 4 h of immersion in SMS and whey protein solution. Corresponding corrosion parameters (average and standard deviation of at least three independent measurements) are compiled in Table 2. With one exception (430 in SMS), all grades remained in their passive state, including three different potential domains; the cathodic domain (potentials below −0.25 V), the passive domain (−0.25–1.25 V) and the transpassive domain at potentials close to 1.25 V. The increased current density at potentials at approximately +1.0 V is related to oxygen evolution [29], and the peak at around +0.75 V is connected to the oxidation of trivalent to hexavalent chromium [30].

In contrast to findings for 430, very similar polarization curves were observed for 2101 and 316 L in SMS, Fig. 3a. From Fig. 3a and Table 2 it can be deduced that grade 2101 exhibited a lower passive current density (≈0.04 μA cm^{-2}) compared to 316 L (≈0.84 μA cm^{-2}) and 430 (2 μA cm^{-2}), indicative of a passive oxide of higher barrier properties on grade 2101. A significant difference observed among the grades was related to their susceptibility for pitting corrosion in SMS. 430 suffered from severe pitting corrosion, whereas no pitting was taking place for either 316 L or 2101, Fig. 3a. These observations were confirmed by post-analysis with LOM, see Fig. 3a.

All grades remained passive in contact with the whey protein solution, Fig. 3b. Similar to the behavior in SMS, grade 2101 revealed the lowest passive current density, followed by 316 L and 430. No pitting corrosion was observed for any grade.

3.4. EIS measurements

Nyquist diagrams and Bode plots are presented in Fig. 4 for the stainless steel grades after 4 h of immersion in SMS and the whey protein solution, respectively. All grades revealed a large semicircle capacitive loop in the Nyquist diagrams, indicative of a typical

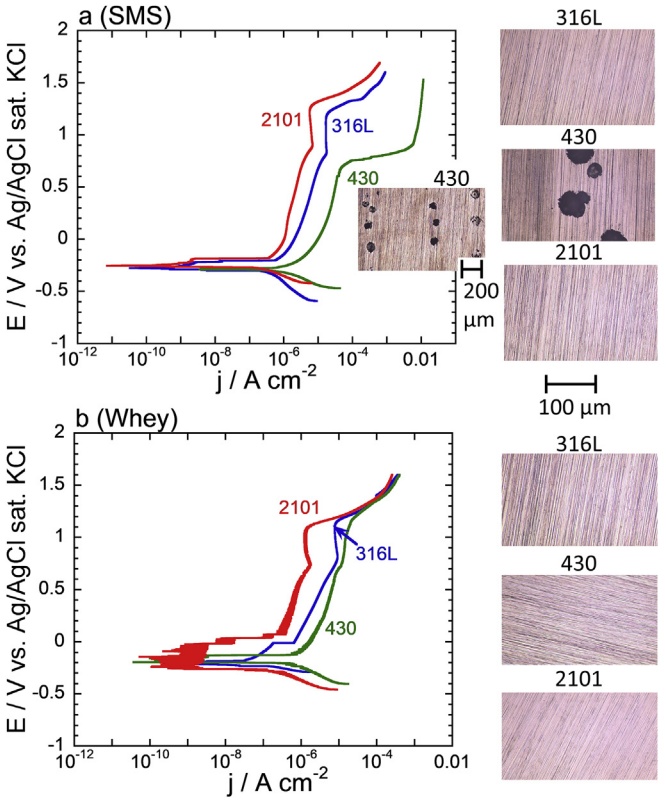

Fig. 3. Representative potentiodynamic polarization curves (scan rate of 1 mV s^{-1}) for 430, 316 L and 2101 after 4 h immersion in SMS (a) and in whey protein solution (b), and corresponding post-polarization light optical microscopy images. Post-polarization images for grade 430 in SMS are shown at two different magnifications.

Table 2
Observed corrosion potentials (E_{corr}/V), passivation current densities (μA cm^{-2}), and breakdown potentials (E_{BP}/V) for 430, 316 L, and 2101 in SMS and in the whey protein solution. The potentials refer to the Ag/AgCl saturated KCl reference electrode. The results reflect mean values and standard deviations of at least three independent measurements for each material and exposure condition. The scan rate was 1 mV s^{-1}.

Solution	Grade	E_{corr} (V)	i_p (μA·cm^{-2})	E_{BP} (V)
SMS	316 L	−0.277 ± 0.01	0.84 ± 0.1	1.13 ± 0.1[a]
	430	−0.315 ± 0.03	2 ± 0.3	0.66 ± 0.05[b]
	2101	−0.255 ± 0.06	0.04 ± 0.01	1.25 ± 0.3[a]
Whey	316 L	−0.190 ± 0.02	0.2 ± 0.05	1.10 ± 0.1[a]
	430	−0.205 ± 0,01	0.9 ± 0.03	1.10 ± 0.1[a]
	2101	−0.145 ± 0.04	0.03 ± 0.01	1.10 ± 0.1[a]

[a] Transpassive breakdown potential.
[b] Pitting potential.

passive state. The impedance results clearly demonstrated the highest passivity for 2101 followed by 316 L and 430 in both solutions. The wide plateau from 10 to 0.1 Hz, with the negative phase angle (-φ) approaching 80° and the log|Z| versus log f slope approximating −1, which was observed in the Bode phase angle curve for 2101 in SMS indicates strong barrier properties of the surface oxide. These barrier properties hinder the migration of aggressive species such as O^{2-} and Cl^{-} from the solution into the alloy interface [31]. Similar observations have been reported for duplex stainless steel (grade 2507) in e.g. seawater [32]. Maximum negative phase values around 80° were recorded for 2101 and 316 L in a broad frequency range (0.01–10 Hz) in the whey protein solution. The maximum negative phase angle was lower for 430 and

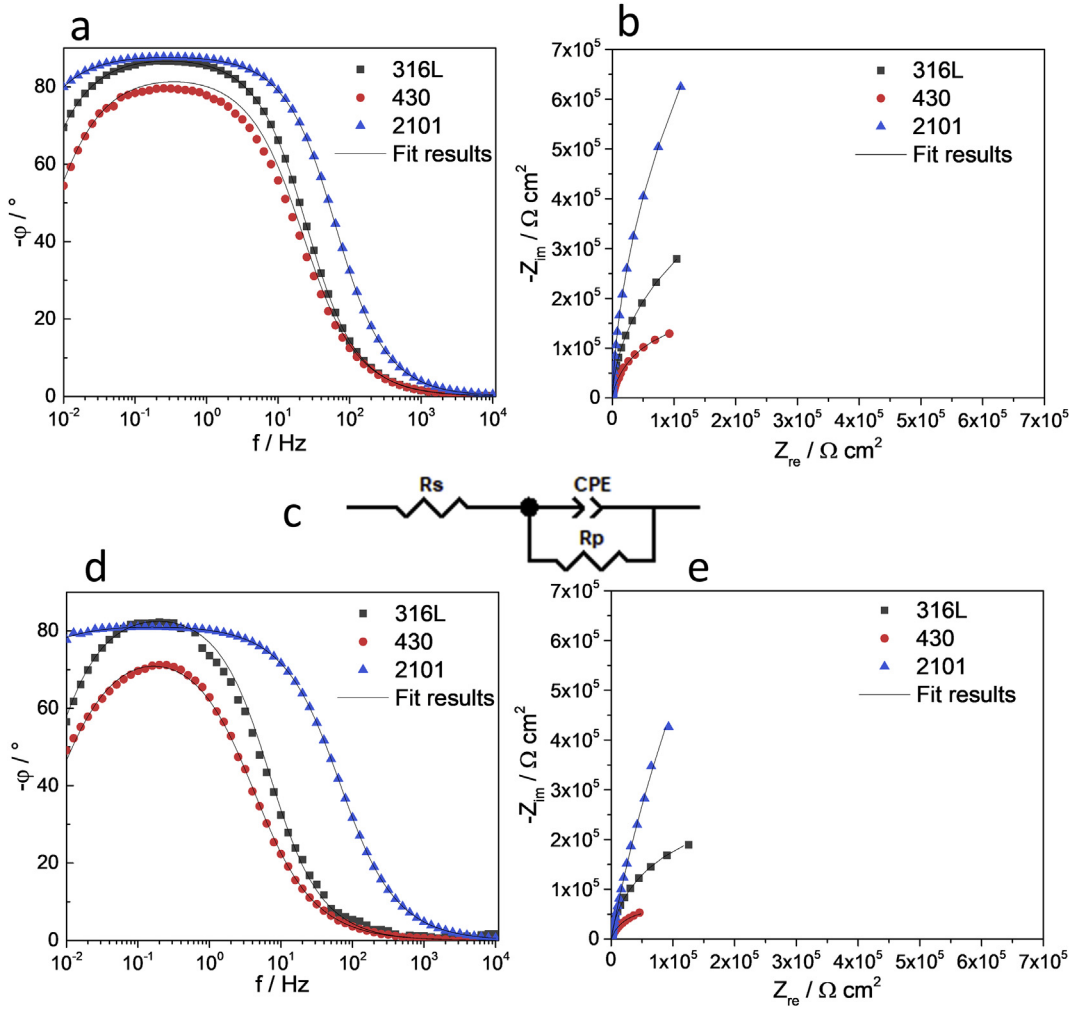

Fig. 4. Nyquist and Bode plots of 316 L, 430, and 2101 after 4 h of immersion in SMS at OCP (a–b) and in whey protein solution (d–e). Data fitted using Randles equivalent electrical circuit (c) in which R_s equals the solution resistance, CPE, the constant phase element and R_p, the polarization resistance.

in a shorter frequency range (0.1–1 Hz) compared with 2101 and 316 L. These results imply that the barrier properties of the passive surface oxide present and formed on 2101 and 316 L were superior compared to the passive surface oxide on 430 in the whey protein solution. Poorer barrier properties of the surface oxide of 430 compared to 2101 and 316 L were also evident in both solutions seen as smaller semicircles and narrower phase plateaus in the Bode plots and Nyquist diagrams.

Since the Nyquist diagrams only exhibited one time constant for all grades, the Randles electrical-equivalent circuit was used, Fig. 4c - f00604c, to fit the EIS data, see experimental section. This model has previously been used for modelling EIS data recorded for stainless steels in the presence of proteins [28,33].

The impedance parameters derived from the EIS fits are compiled in Table 3. According to the chi-squared (χ^2) values, the proposed model successfully fits the EIS experimental results for both solutions, with a better agreement between the measured and simulated values in SMS as compared to the whey protein solution. The results show the largest charge transfer resistance for grade 2101 compared with 316 L and 430, i.e. 2101 to have the best corrosion resistance (lowest corrosion rate) in both SMS and the whey protein solution. Observed differences between the grades were slightly more pronounced in the whey protein solution compared to SMS, Table 3 and Fig. 4. The coefficients of the CPE of 2101 and 316 L were close to 0.9, which means that their behavior was primarily capacitive. The solution resistance was about 2-3-

Table 3
Fitting results of EIS data for 316 L, 430 and 2101 after 4 h immersion in SMS and whey protein solution. Presented results reflect mean values and standard deviation of at least three independent measurements.

Solution	Grade	R_s (Ω cm^2)	CPE (μF cm-2)	R_p (kΩ cm^2)	n	$\chi^2 \times 10^{-4}$
SMS	316 L	149 ± 10	0.51 ± 0.08	932 ± 20	0.97 ± 0.02	<9
	430	165 ± 8	11 ± 10	325 ± 15	0.93 ± 0.02	<8
	2101	195 ± 10	0.35 ± 0.03	4440 ± 120	0.98 ± 0.01	<4
Whey protein solution	316 L	496 ± 5	0.54 ± 0.02	466 ± 10	0.93 ± 0.01	<80
	430	500 ± 12	95 ± 5	132 ± 10	0.83 ± 0.02	<40
	2101	490 ± 6	0.27 ± 0.01	7810 ± 250	0.91 ± 0.01	<0.3

fold greater for all grades in the whey protein solution compared to SMS, Table 3. This is probably mainly related to the lower salt content of the whey protein solution.

3.5. Metal release

Released amounts of Fe, Cr and Ni for the different grades after 0.5, 4, 24 and 48 h in the whey protein solution and in SMS are presented in Fig. 5. A tendency of increased amounts of all metals with time was evident for all grades.

When comparing the total (Fe + Cr + Ni) amount of metal release from the different grades it is evident that 430 released most metals, 1.5–12-fold more than both 316 L and 2101. This was statistically significant ($p < 0.05$) for the release of both Fe and Cr at most time points after 4–48 h of exposure. Significantly less (non-detectable) amounts of Ni were released from 430 compared to the other grades, as expected due to a very low Ni alloy content (<0.1 wt%) in this grade. The released amounts of metals were generally non-proportional to their corresponding bulk alloy composition. This was in particular evident for Fe and Cr released from 2101 to 430 in the whey protein solution for which 98.4% of the total metal release was attributed to Fe (compared to 71–83 wt % Fe in the bulk alloy) and less than 1.5% to Cr (compared to 16–21 wt% Cr in the bulk alloy). These results are related to a higher

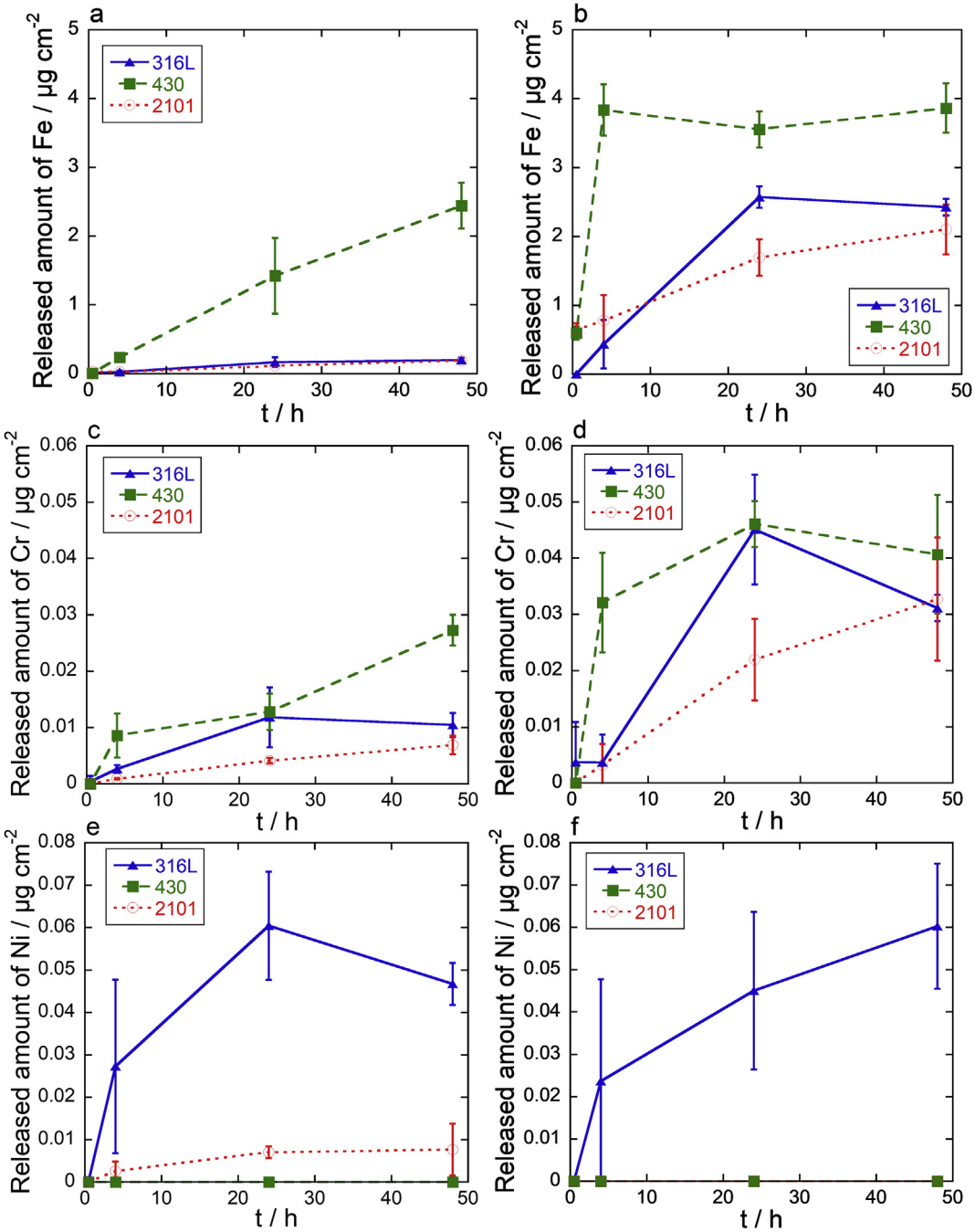

Fig. 5. Released amounts of Fe (a–b), Cr (c–d) and Ni (e–f) from 316 L, 430 and 2101 as a function of exposure time in SMS (a, c, e) and in whey protein solution (b, d, f). The error bars show the standard deviation of independent triplicate coupons. Blank concentrations are subtracted (see experimental section).

solubility of the iron oxide within the passive surface oxide compared to chromium oxide in given conditions [34].

The total amount of released metals, which was dominated by Fe, was for all grades significantly higher (1.6–190-fold) in whey protein solution compared with SMS [statistically significant ($p < 0.05$) for Fe and Cr at most time points, Fig. 5]. This was though not the case for released Ni. No significant increase or decrease of released Ni in whey protein solution compared to SMS were observed for grade 316 L, but a seemingly increased amount of released Ni was observed for 2101 in SMS (detectable amounts) compared to the whey protein solution (non-detectable amounts).

3.6. Surface analysis

The relative fractions of metals (Fe, Cr, and Ni) determined in the outermost surface by means of XPS are compiled in Table 4. Corresponding Fe $2p_{3/2}$, Ni $2p_{3/2}$, and Cr $2p_{3/2}$ spectra are shown in Figs. S1–S2 (supplementary information). Ni was only present in its metallic form and only observed for 316 L at some areas. Fe and Cr were in general observed in both metallic and oxidized forms. As already previously reported for 316 L [11], the exposures in both SMS and whey protein solution resulted in the enrichment of Cr within the surface oxide. There was also a tendency of a reduced oxide thickness upon exposure, indicated by a reduced relative fraction of oxidized to metallic metal constituents within the outermost surface. The ratio of nitrogen (400 ± 0.1 eV) and oxidized carbon (C2: 286.1 ± 0.2 and C3: 288.5 ± 0.2 eV), indicative of proteins [35], to oxidized metal peaks showed evident protein adsorption for all grades. This fraction increased from 21 (unexposed) to 56–63 wt% upon exposure to the whey protein solution for grade 316 L, from 16 to 25–54 wt% for 430, and from 27 to 42–46 wt% for 2101. Consistently, the atomic ratio between nitrogen and oxidized carbon (N/C2+C3) increased from 0.04 to 0.33–0.46 for 316 L, from 0.08 to 0.28–0.36 (except for the 4 h exposure showing undetectable amounts of nitrogen) for 430, and from 0.03 to 0.36–0.57 for 2101.

3.7. Further discussion

Two different mechanisms may explain gradually reduced OCP with time observed for all grades in SMS: *i*) the adsorption of species such as phosphates that reduces the rate of cathodic reactions [28,36], and *ii*) the reduction of surface oxide thickness by complexation with citrate [37–41], which would result in increased anodic reaction rates. XPS results indicate further that the latter may play an important role in SMS. A surface oxide of reduced barrier properties with time combined with the presence of chlorides could further explain the increased pitting susceptibility observed for 430 in SMS compared to its behavior in the whey protein solution. In contrast, the negative shift in OCP with time that was observed for all stainless steel grades in the whey protein solution is most probably associated with protein adsorption, which hinders the cathodic reactions [14,20,21,28,33,36]. These findings were supported by the XPS results. Whether protein adsorption can completely inhibit corrosion of stainless steel on a long-term perspective is debated [25]. However, some studies point out the lack of positive effects after long time periods (reviewed in Ref. [25]). The EIS measurements of this study indicated an influence of protein adsorption on the charge transfer [42]. The results show that adsorption of proteins efficiently hinder corrosion by forming a surface layer. However, the extent of released metals was substantially higher in the whey protein solution as compared to SMS. These observations contrast with the behavior of more actively corroding materials such as iron and mild steel for which the adsorption of proteins has resulted in both reduced extent of corrosion and metal release [21].

Whey proteins consist of about 48–58% β-lactoglobulin, 13–19% α-lactalbumin, 12–20% glycomacropeptide, 6% bovine serum albumin, 8–12% immunoglobulin, 2% lactoferrin, and 0.5% lactoperoxidase [43]. It is very probable that several of these components, especially the albumin and globulin proteins, can increase the extent of protein-induced corrosion by complexation mechanisms [44–46]. The binding sites to these proteins for Cr, Fe, and Ni are

Table 4
Relative fraction (wt.%) of metallic Ni, metallic and oxidized Fe and Cr, and the fraction of oxidic to total metal constituents ($(Fe_{ox} + Cr_{ox})/(Fe_{ox} + Cr_{ox} + Ni_{met} + Fe_{met} + Cr_{met})$ *100 wt%). The results are presented as mean values and standard deviation between measurements on duplicate coupons.

Grade	Solution	Time/h	Ni_{met}	Fe_{met}	Cr_{met}	Fe_{ox}	Cr_{ox}	Oxide fraction
430	–	0	<LOD	14 ± 5	2 ± 0.3	67 ± 2	18 ± 2	84 ± 5
	SMS	0.5	<LOD	13 ± 2	<LOD	62 ± 6	25 ± 5	87 ± 2
	Whey	0.5	<LOD	11 ± 0.2	3 ± 0.9	67 ± 1	19 ± 0.6	86 ± 0.7
		4	<LOD	12 ± 2	<LOD	88 ± 2	<LOD	88 ± 2
		24	<LOD	12 ± 0.7	4 ± 0.2	41 ± 6	42 ± 5	83 ± 0.9
		48	<LOD	21 ± 0.3	2 ± 2	36 ± 2	41 ± 5	77 ± 3
2101	–	0	<LOD	12 ± 0.2	4 ± 0.3	60 ± 2	23 ± 2	86 ± 0.06
	SMS	0.5	<LOD	9 ± 0.2	4 ± 0.3	64 ± 0.4	24 ± 0.2	87 ± 0.6
		4	<LOD	12 ± 0.05	4 ± 0.1	54 ± 1	30 ± 2	84 ± 0.2
		24	<LOD	13 ± 2	5 ± 2	47 ± 2	35±2[a]	82 ± 4
		48	<LOD	14 ± 0.5	4 ± 0.7	43 ± 2	39 ± 0.9[a]	82 ± 1
	Whey	0.5	<LOD	12 ± 1	4 ± 0.1	55 ± 2	28 ± 1	83 ± 1
		4	<LOD	15 ± 2	5 ± 0.4	44 ± 2	36±1[a]	80 ± 1
		24	<LOD	11 ± 1	5 ± 0.7	42 ± 1	41 ± 0.4[a]	84 ± 2
		48	<LOD	19 ± 0.5	5 ± 1	36 ± 3	39±1[a]	75 ± 2
316 L	–	0	2 ± 0.7	8 ± 0.04	2 ± 0.2	70 ± 0.4	19 ± 0.1	89 ± 0.5
	SMS	0.5	1 ± 2	9 ± 3	2 ± 0.2	67 ± 0.9	20 ± 0.08[a]	87 ± 1
		4	2 ± 0.03	6 ± 0.3	2 ± 0.3	69 ± 0.3	21 ± 0.3[a]	90 ± 1
		24	5 ± 2	11 ± 2	2 ± 0.4	49 ± 0.4	33 ± 0.3[a]	82 ± 0.05[b]
		48	5 ± 1	11 ± 0.6	4 ± 0.3	43 ± 0.4	37 ± 0.3[a]	79 ± 0.2[b]
	Whey	0.5	<LOD	6 ± 2	1 ± 0.4	71 ± 4	22 ± 2	93 ± 2
		4	<LOD	7 ± 0.1	2 ± 0.7	60 ± 0.9	31 ± 2	91 ± 0.6
		24	1 ± 1	10 ± 2	2 ± 0.08	48 ± 6	40 ± 5	88 ± 0.8
		48	2 ± 3	11 ± 4	3 ± 0.3	46 ± 0.4	37±1[a]	84 ± 2

[a] Statistically significant ($p < 0.05$) increased amounts compared with unexposed coupons.
[b] Statistically significant ($p < 0.05$) reduced amounts compared with unexposed coupons.

most probably specific and include both strong and weak binding sites [47–49].

The enrichment of Cr in the surface oxide upon exposure of all grades and solutions is consistent with previous findings [2,28,50–52] and with the observed metal release findings. The released amount of Cr compared with the total amount of released metals (Fe + Cr + Ni) was for all grades <5% after 48 h of exposure in SMS and <2% after 48 h in the whey protein solution. Released proportions of Cr were for all grades lower than its corresponding proportion in the bulk alloy (2101–21.4%, 316L-16.9%, 430–16.0%). XPS findings for 316 L imply, in agreement with literature findings [27], Ni to be located beneath the Cr- and Fe-rich surface oxide rather that in the outermost surface oxide. No Ni was observed in the surface oxide of either 2101 or 430 (bulk content 1.5 and < 0.1 wt%, respectively) and was also released to a significantly lower extent compared to 316 L (10.5 wt% Ni in the bulk alloy). The relative release of Ni was 51% of total amount of released metals (Fe + Cr + Ni) for 316 L, and 9% for 2101 after 4 h in SMS. Ni was under these conditions preferentially released compared to its proportion in the bulk alloy (2101–1.6%, 316L-10.1%). This reflects probably the high complexation capacity of the SMS fluid and the concomitant adjustment in composition and barrier properties of the surface oxide [11]. The presence of Ni enriched beneath the surface oxide, here observed for 316 L, has been reported beneficial for the oxidation of Fe and Cr at the metal/oxide interface [53] and may therefore paradoxically result in both a decreased corrosion rate and an increased (initial) release of Ni.

The occurrence of pitting corrosion that was observed for grade 430 during the potentiodynamic polarization in SMS, but not for 2101 or 316 L, is most probably related to an improved corrosion resistance induced by the presence of Mo (316 L) and more Cr (2101) in the bulk alloy for the latter grades, Table 1 [54]. Phosphates in solution have previously been reported to act as corrosion inhibitors towards pitting of different biomedical alloys [33]. The concentration of phosphates in SMS was evidently not sufficient to hinder pitting of grade 430. Similar surface damages due to localized corrosion have previously been reported for grade 430 in chloride-containing food solutions [1]. From the EIS measurements it is evident that the passive surface oxide of grade 430 revealed poorer barrier properties compared to both 316 L and 2101 in both solutions. The lower corrosion rate observed for 2101 compared to 316 L in chloride-containing solutions is consistent with literature findings on another duplex stainless steel grade (2205) at similar conditions [55] and for 2101, compared to different stainless steel grades (among them 316 L and 430), in different food simulants (5 g/L citric acid and artificial tap water) [56]. It has been proposed that duplex stainless steels are new candidate materials to be used within both food industry and in sensitive environments such as the human body [55]. The combination of superior mechanical properties due to the presence of two phases (δ-ferrite and austenite), and an improved corrosion resistance governed by the high Cr bulk content associated with Mo and Ni are the main arguments to encourage the replacement of 316 L with duplex stainless steels [55]. Their specific microstructures result in addition in a dense and homogeneous passive surface oxide [57].

Higher total amounts of released metals from the stainless steel grades into the whey protein solution compared to SMS was not associated with any increased extent of corrosion, rather the opposite with improved surface properties. These observations imply that different mechanisms are prevailing, for example pitting or metastable pitting events were probably not playing any role for any grade at OCP conditions. Furthermore, metal oxidation processes (corrosion) depend only indirectly on adsorption-controlled surface complexation processes with chelating agents (e.g. citrate or proteins), which might be beneficial for the surface oxide adjustment and improved passive properties over time [41]. However, it could also result in a reduced oxide thickness and thereby an increased metal oxidation (corrosion). The rate of complexation-induced release and thereby its effects on the barrier properties of the passive surface oxide depend, among others, on the stability constant of formed complexes, the strength and kinetics of adsorption, the concentration of the chelating agents, prevailing exposure conditions such as rate of agitation, ionic strength (shielding charges), solution pH, and on the presence of other agents/proteins of higher surface binding affinity [24].

This study is limited by its boundary conditions, e.g. the results can only be claimed valid for room temperature and given environments. It has further been conducted without any wear processes taking place, conditions that could result in enhanced extents of metal release and corrosion for certain conditions [11]. However, generated results in this study highlight the importance of stainless steel grade selection and understanding of complexation mechanisms in environments with chelating agents and/or proteins. Finally, it should be noted that released levels of all metals were for all three grades of this study below the specific release limits stipulated by the European Union for alloys in food contact [12], being at least 44-fold lower for Fe, 21-fold lower for Cr, and 10-fold lower for Ni.

4. Conclusions

The aim of this work was to elucidate changes in corrosion behavior, metal release, and surface composition for three grades of stainless steels of different microstructure in a simulated milk solution (SMS) and in a whey protein solution. The studies included austenitic (AISI 316 L), ferritic (AISI 430), and lean duplex (LDX 2101) stainless steels. The following main conclusions were drawn:

1 All grades revealed low corrosion rates (2101 < 316 L < 430) in the whey protein solutions without any sign of active or metastable corrosion.
2 Pitting corrosion events were observed to take place during potentiodynamic polarization of grade 430 in SMS (containing e.g. citrate, chlorides, and phosphates), whereas neither 316 L nor 2101 showed any pitting susceptibility. The corrosion rate in SMS was the highest for 430, followed by 316 L and 2101.
3 Improved passive properties were evident for all grades in both the whey solution and SMS based on the polarization investigations. The EIS findings demonstrated the surface oxide of 2101 to reveal a higher charge transfer resistance and a lower capacitance compared with the surface oxides of both 316 L and 430. The XPS findings showed Cr to be enriched in the surface oxide for all grades upon exposure in both SMS and whey protein solution.
4 In accordance with the electrochemical findings, the total amount of released metals (Fe + Cr + Ni) was highest for grade 430, followed by 316 L and 2101. Most Ni was released from 316 L connected to its presence beneath the surface oxide and a higher bulk alloy content compared with the other grades. Preferential release of Ni compared to its relative bulk content was evident for both 316 L and 2101 in the strongly complexing SMS solution after 4–48 h of exposure. Released amounts of Cr, Ni, and Fe were in all cases substantially lower (10–44 times lower) than stipulated release limits of metals from alloys and metals used in food environments.
5 More metals were released from the different alloys when exposed in the whey protein solution compared to SMS. These findings could not entirely be predicted by the electrochemical measurements, suggesting complexation mechanisms to play an important role.

Funding

Swedish Steel Association - Jernkontoret, Sweden, for a travel grant for Dr. M. Atapour via “Stiftelsen Skandinaviska Malm och Metalls forsknings och utvecklingsfond”.

Author contributions

M.A. conducted the major part of the experiments and drafted the manuscript. I.O.W. conducted the XPS measurements and assisted in drafting the manuscript. Y.H. assisted in experimental design, evaluation, interpretation, drafting, and submission of the manuscript.

Declaration of competing interest

None.

Acknowledgements

Dr. Christofer Lendel is acknowledged for providing the whey proteins and valuable discussions during a previous study. Dr. Gunilla Herting, Dr. Jonas Hedberg, and M. Sc. Xuying Wang are acknowledged for experimental assistance, and Elsa Eriksson, Karin Löfvenborg, and Andreas Renberg are acknowledged for initial experiments during their bachelor thesis at KTH.

Appendix A. Supplementary data

Supplementary data to this article can be found online at https://doi.org/10.1016/j.electacta.2019.135428.

References

[1] D. Steiner Petrovič, D. Mandrino, AES and XPS investigations of the cleaning-agent-induced pitting corrosion of stainless steels used in the food-processing environment, Food Bioprod. Process. 100 (2016) 230–237.
[2] Y.S. Hedberg, I. Odnevall Wallinder, Metal release from stainless steel in biological environments: a review, Biointerphases 11 (2016) 018901-1–018901-17.
[3] M. Henchion, M. Hayes, A.M. Mullen, M. Fenelon, B. Tiwari, Future protein supply and demand: strategies and factors influencing a sustainable equilibrium, Foods 6 (2017) 53.
[4] C. Delgado, M. Rosegrant, H. Steinfeld, S. Ehui, C. Courbois, Livestock to 2020: the next food revolution, Outlook Agric. 30 (2001) 27–29.
[5] M. De Marchi, V. Bonfatti, A. Cecchinato, G. Di Martino, P. Carnier, Prediction of protein composition of individual cow milk using mid-infrared spectroscopy, Ital. J. Anim. Sci. 8 (2009) 399–401.
[6] S. Jovanović, M. Barać, O. Maćej, Whey proteins-properties and possibility of application, (Mljekarstvo: časopis za unaprjeđenje proizvodnje i prerade mlijeka), J. Dairy Prod. Process. Improv. 55 (2005) 215–233.
[7] E. Muehlhoff, A. Bennett, D. McMahon, Milk and Dairy Products in Human Nutrition, Food and Agriculture Organization of the United Nations (FAO), 2013. http://www.fao.org/3/i3396e/i3396e.pdf.
[8] A. Dewangan, A. Patel, A. Bhadania, Stainless steel for dairy and food industry: a review, J. Mater. Sci. Eng. 4 (2015) 1–4.
[9] S. Gupta, S. Anand, Induction of pitting corrosion on stainless steel (grades 304 and 316) used in dairy industry by biofilms of common sporeformers, Int. J. Dairy Technol. 71 (2018) 519–531.
[10] M.S. Jellesen, A.A. Rasmussen, L.R. Hilbert, A review of metal release in the food industry, Mater. Corros. 57 (2006) 387–393.
[11] M. Atapour, Z. Wei, H. Chaudhary, C. Lendel, I. Odnevall Wallinder, Y. Hedberg, Metal release from stainless steel 316L in whey protein- and simulated milk solutions under static and stirring conditions, Food Control 101 (2019) 163–172.
[12] S. Keitel, Metals and Alloys Used in Food Contact Materials and Articles, a Practical Guide for Manufacturers and Regulators, Council of Europe, Strasbourg, France, 2013, ISBN 978-92-871-7703-2.
[13] G. Herting, I. Odnevall Wallinder, C. Leygraf, Corrosion-induced release of chromium and iron from ferritic stainless steel grade AISI 430 in simulated food contact, J. Food Eng. 87 (2008) 291–300.
[14] S. Omanovic, S.G. Roscoe, Electrochemical studies of the adsorption behavior of bovine serum albumin on stainless steel, Langmuir 15 (1999) 8315–8321.
[15] W. Xu, F. Yu, L. Yang, B. Zhang, B. Hou, Y. Li, Accelerated corrosion of 316L stainless steel in simulated body fluids in the presence of H2O2 and albumin, Mater. Sci. Eng. C 92 (2018) 11–19.
[16] S. Karimi, T. Nickchi, A.M. Alfantazi, Long-term corrosion investigation of AISI 316L, Co–28Cr–6Mo, and Ti–6Al–4V alloys in simulated body solutions, Appl. Surf. Sci. 258 (2012) 6087–6096.
[17] I. Frateur, L. Lartundo-Rojas, C. Méthivier, A. Galtayries, P. Marcus, Influence of bovine serum albumin in sulphuric acid aqueous solution on the corrosion and the passivation of an iron–chromium alloy, Electrochim. Acta 51 (2006) 1550–1557.
[18] S. Karimi, A.M. Alfantazi, Electrochemical corrosion behavior of orthopedic biomaterials in presence of human serum albumin, J. Electrochem. Soc. 160 (2013) C206–C214.
[19] G.T. Burstein, C. Liu, Nucleation of corrosion pits in Ringer's solution containing bovine serum, Corros. Sci. 49 (2007) 4296–4306.
[20] Y. Hedberg, M.-E. Karlsson, Z. Wei, M. Žnidaršič, I. Odnevall Wallinder, J. Hedberg, Interaction of albumin and fibrinogen with stainless steel: influence of sequential exposure and protein aggregation on metal release and corrosion resistance, Corrosion 73 (2017) 1423–1436.
[21] Y. Hedberg, X. Wang, J. Hedberg, M. Lundin, E. Blomberg, I. Odnevall Wallinder, Surface-protein interactions on different stainless steel grades: effects of protein adsorption, surface changes and metal release, J. Mater. Sci. Mater. Med. 24 (2013) 1015–1033.
[22] A. Kocijan, I. Milošev, B. Pihlar, The influence of complexing agent and proteins on the corrosion of stainless steels and their metal components, J. Mater. Sci. Mater. Med. 14 (2003) 69–77.
[23] K. Merritt, S.A. Brown, Effect of proteins and pH on fretting corrosion and metal ion release, J. Biomed. Mater. Res. 22 (1988) 111–120.
[24] Y. Hedberg, M.-E. Karlsson, E. Blomberg, I. Odnevall Wallinder, J. Hedberg, Correlation between surface physicochemical properties and the release of iron from stainless steel AISI 304 in biological media, Colloids Surf., B 122 (2014) 216–222.
[25] Y.S. Hedberg, Role of proteins in the degradation of relatively inert alloys in the human body, npj Materials Degradation 2 (2018) 26.
[26] J. Pellier, J. Geringer, B. Forest, Fretting-corrosion between 316L SS and PMMA: influence of ionic strength, protein and electrochemical conditions on material wear. Application to orthopaedic implants, Wear 271 (2011) 1563–1571.
[27] G. Herting, I. Odnevall Wallinder, C. Leygraf, Metal release rate from AISI 316L stainless steel and pure Fe, Cr and Ni into a synthetic biological medium- a comparison, J. Environ. Monit. 10 (2008) 1092–1098.
[28] S. Karimi, T. Nickchi, A. Alfantazi, Effects of bovine serum albumin on the corrosion behaviour of AISI 316L, Co–28Cr–6Mo, and Ti–6Al–4V alloys in phosphate buffered saline solutions, Corros. Sci. 53 (2011) 3262–3272.
[29] C. Vasilescu, P. Drob, E. Vasilescu, I. Demetrescu, D. Ionita, M. Prodana, S.I. Drob, Characterisation and corrosion resistance of the electrodeposited hydroxyapatite and bovine serum albumin/hydroxyapatite films on Ti–6Al–4V–1Zr alloy surface, Corros. Sci. 53 (2011) 992–999.
[30] A.W.E. Hodgson, S. Kurz, S. Virtanen, V. Fervel, C.O.A. Olsson, S. Mischler, Passive and transpassive behaviour of CoCrMo in simulated biological solutions, Electrochim. Acta 49 (2004) 2167–2178.
[31] W. Hu, J. Xu, X. Lu, D. Hu, H. Tao, P. Munroe, Z.-H. Xie, Corrosion and wear behaviours of a reactive-sputter-deposited Ta2O5 nanoceramic coating, Appl. Surf. Sci. 368 (2016) 177–190.
[32] Z. Cui, S. Chen, Y. Dou, S. Han, L. Wang, C. Man, X. Wang, S. Chen, Y.F. Cheng, X. Li, Passivation behavior and surface chemistry of 2507 super duplex stainless steel in artificial seawater: influence of dissolved oxygen and pH, Corros. Sci. 150 (2019) 218–234.
[33] C. Valero Vidal, A. Igual Muñoz, Electrochemical characterisation of biomedical alloys for surgical implants in simulated body fluids, Corros. Sci. 50 (2008) 1954–1961.
[34]] J.E. Castle, J.H. Qiu, Ion selectivity in the passivation of a Ni bearing steel, Corros. Sci. 30 (1990) 429–438.
[35] B. Wu, C. Mu, G. Zhang, W. Lin, Effects of Cr3+ on the structure of collagen fiber, Langmuir 25 (2009) 11905–11910.
[36] Y.-C. Tang, S. Katsuma, S. Fujimoto, S. Hiromoto, Electrochemical study of Type 304 and 316L stainless steels in simulated body fluids and cell cultures, Acta Biomater. 2 (2006) 709–715.
[37] H.H. Hassan, Effect of chloride ions on the corrosion behaviour of steel in 0.1M citrate, Electrochim. Acta 51 (2005) 526–535.
[38] H. Harms, H.-P. Volkland, G. Repphun, A. Hiltpolt, O. Wanner, A.J.B. Zehnder, Action of chelators on solid iron in phosphate-containing aqueous solutions, Corros. Sci. 45 (2003) 1717–1732.
[39] S. Modiano, C.S. Fugivara, A.V. Benedetti, Effect of citrate ions on the electrochemical behaviour of low-carbon steel in borate buffer solutions, Corros. Sci. 46 (2004) 529–545.
[40] L.V. Kremer, Improvements in passivation using citric acid formulations, in: Medical Device Materials: Materials & Processes for Medical Devices Conference, ASM International Materials Park, OH, 2004, p. 87.
[41] N. Mazinanian, Y.S. Hedberg, Metal release mechanisms for passive stainless steel in citric acid at weakly acidic pH, J. Electrochem. Soc. 163 (2016) C686–C693.
[42] N.P. Cosman, K. Fatih, S.G. Roscoe, Electrochemical impedance spectroscopy study of the adsorption behaviour of α-lactalbumin and β-casein at stainless steel, J. Electroanal. Chem. 574 (2005) 261–271.
[43] M. Guo, G. Wang, Whey protein polymerisation and its applications in

environmentally safe adhesives, Int. J. Dairy Technol. 69 (2016) 481–488.
[44] M. Lundin, Y. Hedberg, T. Jiang, G. Herting, X. Wang, E. Thormann, E. Blomberg, I. Odnevall Wallinder, Adsorption and protein-induced metal release from chromium metal and stainless steel, J. Colloid Interface Sci. 366 (2012) 155–164.
[45] J.L. Woodman, J. Black, S.A. Jiminez, Isolation of serum protein organometallic corrosion products from 316LSS and HS-21 in vitro and in vivo, J. Biomed. Mater. Res. 18 (1984) 99–114.
[46] K. Merritt, S. Brown, N. Sharkey, The binding of metal salts and corrosion products to cells and proteins in vitro, J. Biomed. Mater. Res. 18 (1984) 1005–1015.
[47] C. Tkaczyk, O.L. Huk, F. Mwale, J. Antoniou, D.J. Zukor, A. Petit, M. Tabrizian, Investigation of the binding of Cr(III) complexes to bovine and human serum proteins: a proteomic approach, J. Biomed. Mater. Res. A 94A (2010) 214–222.
[48] J.A. Tainer, V.A. Roberts, E.D. Getzoff, Protein metal-binding sites, Curr. Opin. Biotechnol. 3 (1992) 378–387.
[49] Y.S. Hedberg, I. Dobryden, H. Chaudhary, Z. Wei, P. Claesson, C. Lendel, Synergistic effects of metal-induced aggregation of human serum albumin, Colloids Surf., B 173 (2019) 751–758.
[50] F. Di Franco, M. Santamaria, G. Massaro, F. Di Quarto, Photoelectrochemical monitoring of rouging and de-rouging on AISI 316L, Corros. Sci. 116 (2017) 74–87.
[51] W. Fredriksson, S. Malmgren, T. Gustafsson, M. Gorgoi, K. Edström, Full depth profile of passive films on 316L stainless steel based on high resolution HAXPES in combination with ARXPS, Appl. Surf. Sci. 258 (2012) 5790–5797.
[52] H. Xu, L. Wang, D. Sun, H. Yu, The passive oxide films growth on 316L stainless steel in borate buffer solution measured by real-time spectroscopic ellipsometry, Appl. Surf. Sci. 351 (2015) 367–373.
[53] M.J. Carmezim, A.M. Simões, M.F. Montemor, M.D. Cunha Belo, Capacitance behaviour of passive films on ferritic and austenitic stainless steel, Corros. Sci. 47 (2005) 581–591.
[54] J.M. Bastidas, C.L. Torres, E. Cano, J.L. Polo, Influence of molybdenum on passivation of polarised stainless steels in a chloride environment, Corros. Sci. 44 (2002) 625–633.
[55] M. Conradi, P.M. Schön, A. Kocijan, M. Jenko, G.J. Vancso, Surface analysis of localized corrosion of austenitic 316L and duplex 2205 stainless steels in simulated body solutions, Mater. Chem. Phys. 130 (2011) 708–713.
[56] N. Mazinanian, G. Herting, I. Odnevall Wallinder, Y. Hedberg, Metal release and corrosion resistance of different stainless steel grades in simulated food contact, Corrosion 72 (2016) 775–790.
[57] E. Gardin, S. Zanna, A. Seyeux, A. Allion-Maurer, P. Marcus, XPS and ToF-SIMS characterization of the surface oxides on lean duplex stainless steel – global and local approaches, Corros. Sci. 155 (2019) 121–133.